Assessing the temporal variability in extreme storm-tide time series for coastal flood risk assessment

Quinn, N.; Lewis, Matthew; Wadey, M.P.; Haigh, I.D.

Journal of geophysical research:Oceans

DOI:
10.1002/2014JC010197
10.1002/2014JC010197

Published: 11/08/2014

AGU PUBLICATIONS

JGR

Journal of Geophysical Research: Oceans

RESEARCH ARTICLE

10.1002/2014JC010197

Key Points:

- Extreme storm-tide time series variability is examined along the UK coastline
- Variability is shaped by site location and time relative to high water
- Time series uncertainty can have significant impacts on flood risk predictions

Correspondence to:
N. Quinn,
Niall.Quinn@Bristol.ac.uk

Citation:
Quinn, N., M. Lewis, M. P. Wadey, and I. D. Haigh (2014), Assessing the temporal variability in extreme storm-tide time series for coastal flood risk assessment, *J. Geophys. Res. Oceans*, *119*, 4983–4998, doi:10.1002/2014JC010197.

Received 30 MAY 2014
Accepted 16 JUL 2014
Accepted article online 22 JUL 2014
Published online 11 AUG 2014

Assessing the temporal variability in extreme storm-tide time series for coastal flood risk assessment

N. Quinn[1], M. Lewis[2], M. P. Wadey[3], and I. D. Haigh[3]

[1]School of Geographical Sciences, University of Bristol, Bristol, UK, [2]School of Ocean Sciences, Bangor University, Menai Bridge, UK, [3]Ocean and Earth Science, National Oceanography Centre, University of Southampton, Southampton, UK

Abstract The probability of extreme storm-tide events has been extensively studied; however, the variability within the duration of such events and implications to flood risk is less well understood. This research quantifies such variability during extreme storm-tide events (the combined elevation of the tide, surge, and their interactions) at 44 national tide gauges around the UK. Extreme storm-tide events were sampled from water level measurements taken every 15 min between 1993 and 2012. At each site, the variability in elevation at each time step, relative to a given event peak, was quantified. The magnitude of this time series variability was influenced both by gauge location (and hence the tidal and nontidal residual characteristics) and the time relative to high water. The potential influence of this variability on coastal inundation was assessed across all UK gauge sites, followed by a detailed case study of Portsmouth. A two-dimensional hydrodynamic model of the Portsmouth region was used to demonstrate that given a current 1 in 200 year storm-tide event, the predicted number of buildings inundated differed by more than 30% when contrasting simulations forced with the upper and lower bounds of the observed time series variability. The results indicate that variability in the time series of the storm-tide event can have considerable influence upon overflow volumes, hence with implications for coastal flood risk assessments. Therefore, further evaluating and representing this uncertainty in future flood risk assessments is vital, while the envelopes of variability defined in this research provides a valuable tool for coastal flood modelers.

1. Introduction

Coastal areas are heavily populated regions throughout the world; more than a billion people and a significant portion of the global gross domestic product (GDP) are found within 100 km of the coast [*Small and Nicholls*, 2003]. Over recent decades, coastal populations have continued to grow much more rapidly than global mean populations, particularly in less developed countries [*Spencer and French*, 1993; *Hunt*, 2005]. Continued urbanization and migration is expected to significantly increase the value of assets found near coasts in the coming century [*Nicholls*, 1995; *Turner et al*., 1996; *Zong and Tooley*, 2003; *Mokrech et al*., 2012]. Given that 14 out of the world's 17 recognized global megacities (with populations exceeding 10 million) are located in coastal zones [*Tibbetts*, 2002; *Sekovski et al*., 2012]; accurately assessing flood risk to these densely populated regions is of critical importance for coastal communities and to guide adaption strategies.

Storm tides are the total still (i.e., excluding waves) water levels experienced at the coast due to the combination of three main factors: (1) mean sea level; (2) astronomical tide; and (3) storm surge [*Pugh*, 2004; *Lewis et al*., 2011] and can result in devastating coastal floods due to the large number of people and assets in low-lying coastal regions found throughout the world. For example, more than 440,000 people were killed in two storm-tide events occurring in 1970 and 1991 in the Bay of Bengal alone [*Flather*, 1994], while Hurricane Katrina [e.g., *Risk Management Solutions*, 2005] and Hurricane Sandy have recently caused devastation on the U.S. coastline. More recently, Typhoon Haiyan, which hit the Philippines in November 2013, induced a storm tide of more than 25 ft (7.6 m) which affected more than 14 million people, causing about 6200 deaths [*Barmania*, 2014; see also http://reliefweb.int/disaster/tc-2013-000139-phl for more information).

Efficient planning and resource allocation is essential in order to cope with current risk, and the likely increase in risk facing many areas due to rising mean sea levels in the coming century [*Houghton*, 2005; *Meehl et al*., 2007; *Lowe et al*., 2009; *Haigh et al*., 2011]. Furthermore, due to the temporal lead time required to construct mitigation strategies and flood defenses, an accurate assessment of the spatial and temporal changes to risk (here defined as the product of the probability and consequences of flooding) is vital and imminently required. An important component of this process is accurate risk-based assessments to inform policy decisions. Typically this is achieved using a numerical modeling approach in which storm-tide conditions of interest, commonly based on a probability of exceedence or "return period" [e.g., *Tawn*, 1992; *Haigh et al*., 2010], are imposed upon an inundation model domain boundary [e.g., *Bates et al*., 2005, 2010], which may incorporate defense responses and be used to assess economic damage [e.g., *Dawson et al*., 2009]. Resulting flood conditions may be used to infer likely inundation extents and potential losses for specific flood events [e.g., *Stansby et al*., 2012; *Smith et al*., 2012; *Wadey et al*., 2012). These assessments provide a vital tool for informing policy decisions (e.g., cost-benefit of flood defenses; shoreline planning) and scenario-based assessment of coastal change [*Dawson et al*., 2003]. However, errors are inevitably introduced into model predictions through a variety of sources including inaccurate estimates of initial conditions, inaccurate boundary forcing, and lack of complete knowledge of the system leading to an inability of numerical models to fully represent many physical processes [*Maybeck*, 1979; *Madsen and Canizares*, 1999; *Kantha and Clayson*, 2000; *Brown et al*., 2007; *Neal*, 2007]. Such uncertainties will impact both deterministic and probabilistic predictions of inundation extent and depth. The ultimate result is divergence from reality in the model predictions. Understanding this uncertainty is essential as unrealistic expectations of accuracy can result in the misinterpretations of flood risk, with profound implications [*Brown and Damery*, 2002; *Hall and Solomatine*, 2008]. For this reason, many operational forecasting systems and risk assessments provide probabilistic predictions in an attempt to explicitly account for known uncertainties in the modeling approach used [e.g., *Purvis et al*., 2008; *Bocquet et al*., 2009; *Pappenberger and Beven*, 2006; *Davis et al*., 2010; *Kim et al*., 2010].

A fundamental source of uncertainty in various coastal-based numerical models and empirical approaches used to predict coastal events and change (e.g., flooding, sediment transport, and erosion) is the specification of the tide and surge boundary conditions. Model sensitivity due to this input is high, due to its fundamental influence upon the volume and rate at which water enters the model domain (and can then be distributed). It has been established that astronomical tidal elevations are often not predicted well by physically based numerical models (particularly in complex nearshore regions); hence, harmonic tide predictions (based on measured data) are substituted in the place of outputs from such models in many operational systems due to their greater accuracy [*Bocquet et al*., 2009; *Flowerdew et al*., 2009]. Furthermore, meteorically induced storm surges, tide-surge interaction effects causing phase variation, and local conditions (e.g., bathymetry) complicate combined tide and surge predictions (which we call storm tide). Recently, progress has been made in forecasting extreme storm tides around complex coastlines allowing for more accurate estimates between gauged locations [*Horsburgh et al*., 2008; *Lewis et al*., 2011, 2013] and in the prediction of the heights and probabilities of extreme sea levels [*McMillan et al*., 2011; *Batstone et al*., 2013; *Haigh et al*., 2014a, 2014b).

Typically an idealized storm-tide time series (often derived from a previously observed event) is applied to these return level estimates to force an inundation model at a given location [e.g., *Dawson et al*., 2005; *Purvis et al*., 2008; *McMillan et al*., 2011; *Batstone et al*., 2013; *Gallien et al*., 2011; *Quinn et al*., 2013]. However, the true storm-tide time series is likely to vary spatially (along a section of coastline) and temporally (between subsequent events), even for a given event magnitude, due to variability in tide and surge characteristics, and the complexity of their interactions [*Horsburgh and Wilson*, 2007; *Wolf*, 2009; *Brown et al*., 2011; *Lewis et al*., 2013]. No two storm-tide events are the same, because different combinations of tide and surge (superimposed on different mean sea levels) combine to give the total water levels observed during events. For example, Figure 1 shows time series of total water level at Liverpool for eight events, and the corresponding time series of tide and nontidal residual that combine to give the total water levels for those eight events. The nontidal residual is the difference in elevations relative to those generated by the tide alone and primarily contains the surge and tide-surge interaction effects [*Pugh*, 1987; *Horsburgh and Wilson*, 2007]. For each of the eight events, the maximum water level is 10.37 m Chart Datum (which corresponds to a 1 in 2 year return period). But what is clear from Figure 1 is that the temporal variability in the hours leading up to and then proceeding the peak water level of each of these eight events is different, because of differences in the tidal and nontidal residual time series. This uncertainty in the storm-tide time series is not commonly quantified in coastal flood risk assessments, and hence is the focus of our study.

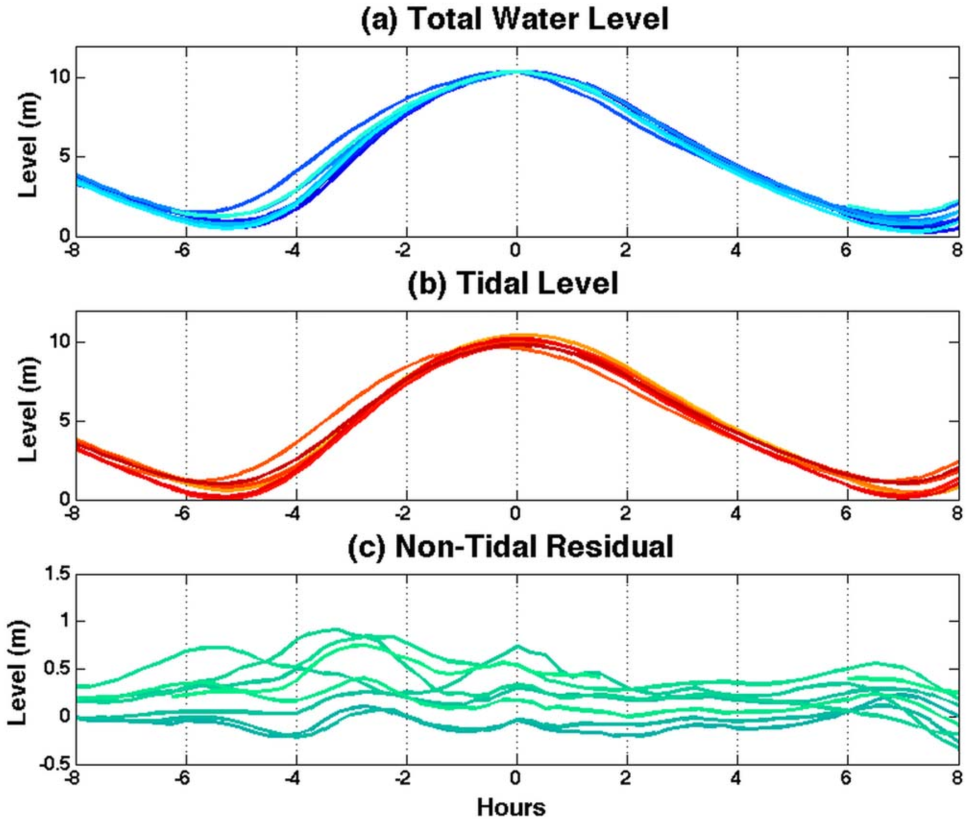

Figure 1. Time series of total water level, tidal, and nontidal residual at Liverpool for eight storm-tide events whose maximum water level is comparable.

Uncertainty in the true time series of a storm-tide event, particularly close to the time of high water (when defense exceedance is most likely) may lead to uncertainty in the duration (and therefore volume) of water affecting a region of interest; a factor currently not considered systematically in many flood risk assessments. This will have important implications on the simulated inundation extent and depth, and thus the predicted risk. Further, the probability of defense failure is likely to increase the longer a peak water level persists, while other processes of relevance to flood risk such as wave-overtopping and erosion of beaches and soft defenses would also be expected to respond to changes in the storm-tide time series [e.g., *Pullen et al*., 2007; *Roelvink et al*., 2009].

Therefore, the first objective of this paper is to define the uncertainty within such an assumption by quantifying the natural observed variability in extreme storm-tide time series around the UK; a region that has a long history of coastal flooding, particularly from surges occurring in the North Sea [e.g., *Gönnert et al*., 2001; *McRobie et al*., 2005; *Baxter*, 2005; *Gerritsen*, 2005]. Most recently, throughout December 2013 to February 2014, many areas of the UK experienced a sequence of severe storm events, leading to thousands of homes being flooded and many more evacuated [*Slingo et al*., 2014]. This information will be useful to better inform future flood risk assessments. The magnitude of the variability in storm-tide time series is assessed around the UK in order to ascertain site characteristics that are prone to induce a high level of uncertainty in an extreme storm-tide time series; information that will be of value to policy makers and modelers interested in coastal flood risk. The second objective of the paper is to examine the implications of the variability observed in the storm-tide time series at different sites. We do this by undertaking a theoretical assessment of overflow volumes (where still water levels exceed defense elevations) at each gauge site, and also carry out a case study sensitivity analysis of flood inundation at Portsmouth, one of the most flood prone cities in the UK.

The paper is formatted as follows: section 2 introduces the study sites and data sets; section 3 describes the methods used to define the variability in storm-tide time series and examine its significance to flood risk; the results and discussion are presented in section 4; while the conclusions are given in section 5.

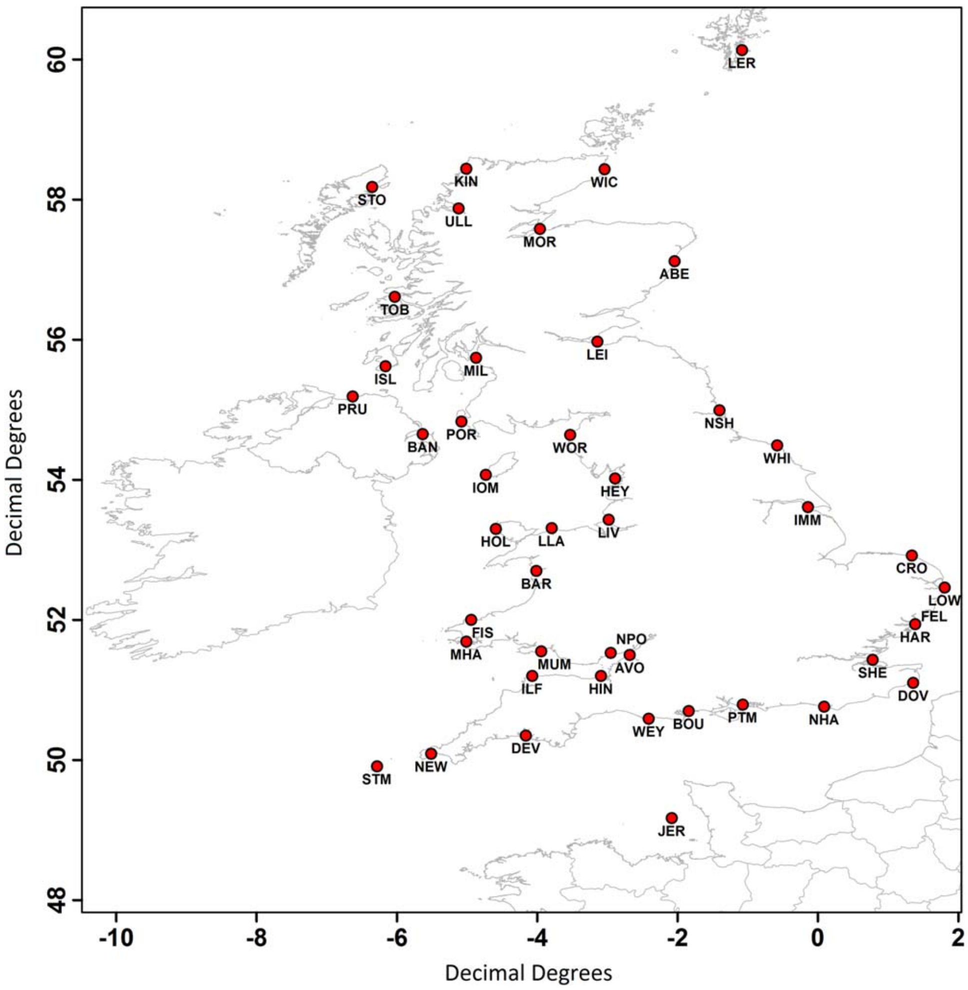

Figure 2. Tide gauge sites used in the analysis.

2. Sea Level Data Sets

This research focused on water level time series measured across the comprehensive UK national A-Class tide gauge database (Figure 2 and Table 1). Water level measurements at 15 min temporal resolution were obtained for 44 sites around the UK from the British Oceanographic Data Centre (BODC, www.bodc.ac.uk), who archive and quality control the data on behalf of the National Tidal and Sea Level Facility (www.ntslf.org). To ensure results were comparable between sites, the focus was only on the 20 year period from 1993 to 2012. All sites contained at least 15 years of data for this period with the exception of Harwick, Lerwick, and Moray Firth, which included 8, 14, and 10 years, respectively. All data archived by the BODC has undergone quality control and corresponding quality markers are recorded, which were used to remove any potentially erroneous data prior to analysis.

As the focus is on comparing extreme storm tides, we removed the mean sea level component from the measured water level data sets and then separated the time series into an astronomical tidal component and a nontidal residual. To isolate the contribution of sea level changes caused by individual storm events (rather than longer term seasonal or interannual changes in meteorology), the MSL component (indicative of seasonal, interannual, and longer term change) was derived using a 30 day running mean of the observed sea level time series at each site, and this was subsequently removed from the record for that site. Harmonic analysis was performed with T-Tide [*Pawlowicz et al.*, 2002] for each calendar year with the standard set of 67 tidal constituents, to predict the tidal component. The nontidal residual was determined by subtracting the calculated tidal component from the measured time series.

Table 1. Tide Gauge Information

		Location (Decimal Degrees)		
Station Name	Site ID	Latitude	Longitude	Data Length (Years)
Aberdeen	ABE	57.14	−2.08	19
Avonmouth	AVO	51.52	−2.72	19
Bangor	BAN	54.67	−5.67	18
Barmouth	BAR	52.72	−4.05	19
Bournemouth	BOU	50.72	−1.88	16
Cromer	CRO	52.94	1.3	19
Devonport	DEV	50.37	−4.2	19
Dover	DOV	51.12	1.32	19
Felixstowe	FEL	51.96	1.35	18
Fishguard	FIS	52.02	−4.98	19
Harwich	HAR	51.96	1.35	8
Heysham	HEY	54.04	−2.93	19
Hinkley Point	HIN	51.22	−3.13	19
Holyhead	HOL	53.32	−4.63	17
Ilfracombe	ILF	51.22	−4.11	19
Immingham	IMM	53.63	−0.18	19
Jersey	JER	49.19	−2.12	19
Kinlochbervie	KIN	58.46	−5.05	19
Leith	LEI	55.99	−3.18	19
Lerwick	LER	60.15	−1.12	14
Liverpool	LIV	53.45	−3.02	19
Llandudno	LLA	53.33	−3.83	18
Lowestoft	LOW	52.48	1.77	19
Milford Haven	MHA	51.71	−5.05	19
Millport	MIL	55.76	−4.91	19
Moray Firth	MOR	57.6	−4	10
Mumbles	MUM	51.57	−3.98	19
Newhaven	NHA	50.78	0.05	19
Newlyn	NEW	50.11	−5.55	19
Newport	NPO	51.55	−2.99	19
North Shields	NSH	55.01	−1.44	19
Port Ellen	ISL	55.64	−6.2	18
Port Erin	IOM	54.09	−4.77	19
Portpatrick	POR	54.85	−5.12	19
Portrush	PRU	55.21	−6.67	17
Portsmouth	PTM	50.81	−1.11	17
St. Mary's	STM	49.93	−6.32	18
Sheerness	SHE	51.45	0.74	19
Stornoway	STO	58.2	−6.39	19
Tobermory	TOB	56.63	−6.07	15
Ullapool	ULL	57.89	−5.16	15
Weymouth	WEY	50.61	−2.45	19
Whitby	WHI	54.51	−0.62	19
Wick	WIC	58.45	−3.08	15
Workington	WOR	54.66	−3.57	16

3. Methods

3.1. Variability in the Storm-Tide Event Time Series

The first study objective is to quantify the variability during extreme storm-tide event time series, particularly in the hours leading up to and then proceeding the peak water level of events. To do this a representative set of extreme storm-tide event time series was selected from the available data at each site. Using this selected ensemble of events, the spread (variability) in the water level elevations, every 15 min, over a 12 h event time window, centered on time of maximum water level, was examined and used to define a representative mean, upper and lower storm-tide time series, which captures the envelope of variability at each site.

Preliminary analysis indicated that the data selection criterion was influential upon the resulting ensemble, and therefore, the estimate of time series variability. Relaxing the high water constraint (thereby including a greater number of events) at a site was found to result in a larger spread in the ensemble at any given time step. As this research was primarily interested in quantifying the variability in extreme storm-tide time series

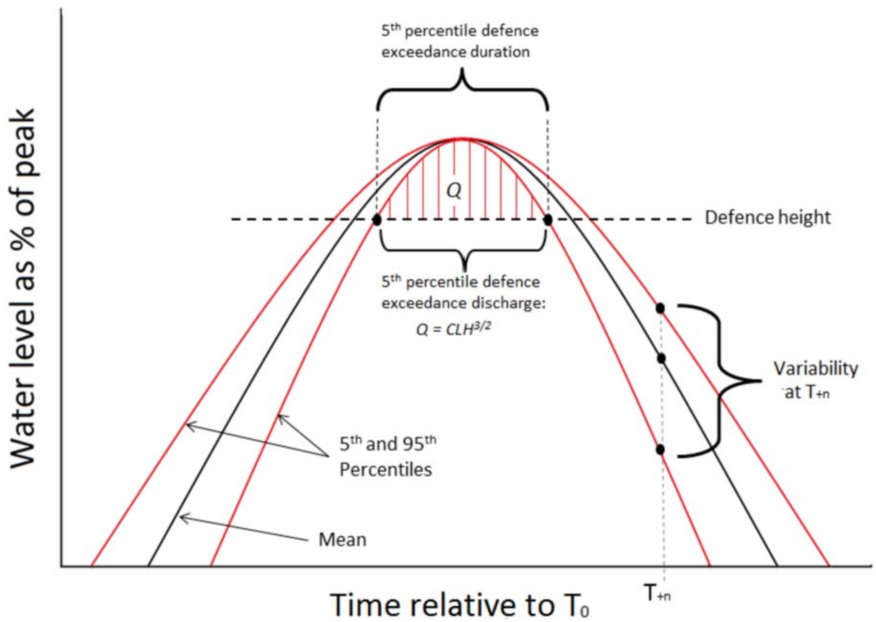

Figure 3. Ensemble statistics used to quantify event time series uncertainty.

and its potential impacts on flood risk, only the largest 1% of events was used at each site. This enabled the research to focus on defining the time series variability in the largest events, which will be of most interest to flood risk managers, while allowing for adequately large ensembles (between 100 and 150 events) to still be considered at each site.

The following steps were used at each site shown in Figure 2:

1. Every high water was identified from the available data, and all but the largest 1% were discarded.

2. The remaining high water points were used as index points to extract the total water level, tide, and non-tidal residual elevations 6 h either side of the peak, at 15 min resolution.

3. Considering the ensemble of time series; the standard deviation, mean, 95th and 5th percentile statistics at each time step were then calculated.

4. For each event, the water level at each time step was calculated as a proportion of the event peak to allow comparison of the time series shape between events more easily. The same statistics calculated in step (c) were then extracted from the new normalized ensemble of time series.

The standard deviation in the tide, nontidal residuals, and total water level ensembles at each time step was used as a primary indicator of variability of the storm-tide time series; representing the spread in elevations at a time step, given as a proportion of the event peak magnitude. The ensemble mean, 95th and 5th percentile time series provided the upper and lower bounds on the likely shape of an extreme storm-tide time series at a given site (Figure 3).

3.2. Influence of Time Series Uncertainty on Coastal Inundation

The second objective of the paper is to examine some of the implications of the variability in the storm-tide time series defined in objective 1. To do this, two sets of analysis were made: a theoretical assessment of overflow volumes at each site and a detailed local analysis of the impact on flooding inundation extent at Portsmouth.

To examine the potential implications upon defense overflow volumes at the gauge sites, the peak storm-tide heights with a 1 in 300, 500, and 1000 year probability of exceedance were selected [estimated by *McMillan et al*., 2011 for the UK Environment Agency], and the uncertainty associated with the water level time series of these events investigated. The upper and lower bounds of the variability envelopes defined in section 3.1 (Figure 3) were used to define two event time series for each of the selected event magnitudes, at each site.

At each site, a hypothetical sea defense built to a 1 in 200 year level standard was defined [the standard for approximately 400,000 homes in the UK coastal zone; *Committee on Climate Change*, 2013] and the constructed storm-tide time series were used to estimate overflow volumes during the event. The flow of water over the defense was represented by broad crested weir equations [*Ackers et al*., 1978; *Quinn et al*., 2013]. Given these conditions, the volume of discharge (per unit length of defense) was calculated every 15 min, and the total event discharge was given as the sum of all time steps. In this example, the water level in a given bin was assumed to be static for the 15 min duration of the bin. The total event discharge can be represented by

$$Q_T=\sum_{i=1}^{n} Q_i$$

where Q_T is the total event discharge, and the discharge in bin i, Q_i, is given by

$$Q_i=CLH_i^{\frac{3}{2}}$$

where *C* is a weir coefficient (given as 1.5), *L* is the length (1 m), and *H* is the water head (m).

Four sites away from Mainland UK (Bangor, Harwich, Saint Helier, and Portrush) were not included in this portion of the analysis because return period statistics were not available for them [*McMillan et al*., 2011; *Batstone et al*., 2013].

To provide a more detailed example of the potential impacts of time series variability upon extreme events, a two-dimensional (2-D) inundation case study was also undertaken for the low-lying and densely populated UK city of Portsmouth which is ranked only behind London and Hull for the amount of property at risk of coastal flooding [*RIBA and ICE*, 2009]. The city is surrounded by hard defense structures, most of which are expected to provide approximately a 1 in 200 year standard of protection. The flood simulation method comprised point vectors placed onto the edge of a digital elevation model (DEM), with each point associated with a storm-tide water level time series. The DEM was assembled from LiDAR data collected between 2007 and 2008 by the Environment Agency (EA) at 1–2 m resolution. This was spatially averaged to 50 m cells. For the case study of Portsmouth, this resulted in 150 columns and 168 rows of cells, in the form of a regular grid. The vertical root-mean-square-error of the LiDAR collected by the EA was within $\pm$0.10 m of the available ground-based check points. Flood water was propagated inland using the 2-D raster based inundation model LISFLOOD-FP [refer to *Bates et al*., 2010 for technical details of this model]. The coarse scale is acknowledged in this example for urban flood modeling: finer resolution grids can generate more accurate representations of flow diverting around buildings, while less interpolation of the original topographic survey data can allow a more realistic approximation of floodplain water depths [*Fewtrell et al*., 2008]. However, the modeling method has been validated against real floods in nearby areas [*Wadey et al*., 2012, 2013] and is hence considered to be sufficient to demonstrate the effects of different storm tides on basic coastal flood predictions. Two defense conditions scenarios were simulated:

1. **No breach**—Defense crest heights collected by ground-based surveys with $\pm$0.03 m accuracy were appended to the DEM. The storm-tide water level time series was routed over these defenses which were assumed to hold.

2. **Breach**—Defense structures were removed from the DEM and water was able to flow into the domain if the land height behind the defense was lower than the inflow boundary water level. Although breaching is unlikely to occur in such a drastic manner, agencies such as the EA often define flood maps under such conditions (e.g., http://apps.environment-agency.gov.uk/wiyby/37837.aspx).

Wave-overtopping was excluded due to the high uncertainties described in previous studies, especially when linked to inundation simulations [e.g., *Pullen et al*., 2007, 2009; *Smith et al*., 2012] although more recent research has reported prediction accuracies of approximately 20% when compared to field data [*McCabe et al*., 2013]. Furthermore, Portsmouth has not experienced a major coastal flood in recent years, and it was not possible to calibrate the wave-overtopping predictions. Surface friction, parameterized within the LISFLOOD-FP kinematic wave equation as the Manning's *n* roughness coefficient [see *Bates et al*., 2010],

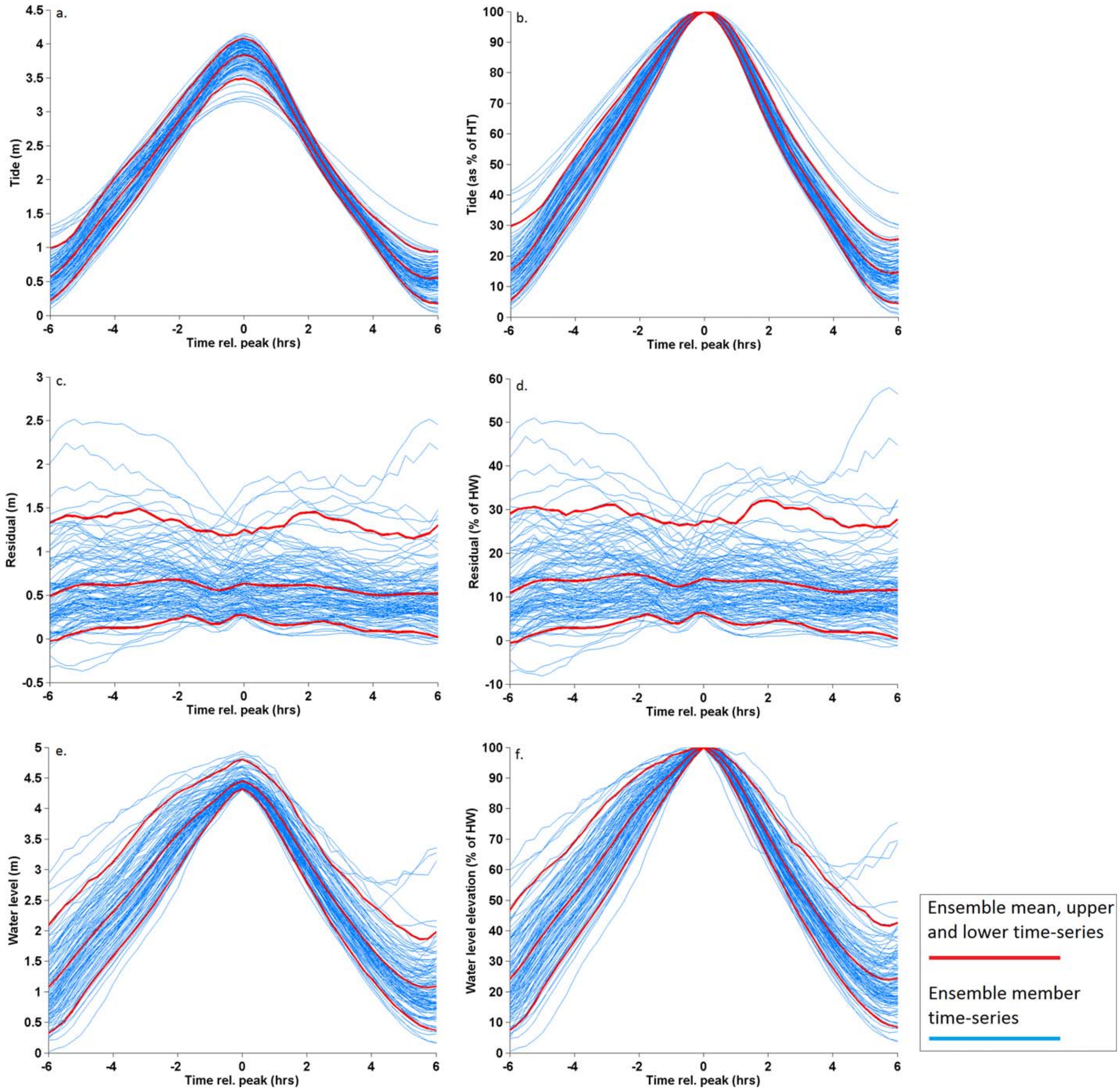

Figure 4. Tide, residual, and water levels associated with the top 1% of storm-tide events at Felixstowe. (a) Absolute tide, (c) residual, and (e) water level elevations. (b) Tidal elevation relative to high tide, while (d) residual elevations and (f) water level elevations relative to peak water.

was set at a spatially homogenous value of 0.035, while the time step was set within the model to optimize stability and computational efficiency.

Water level peaks representing 1 in 1, 10, 50, 200, 300, 500, and 1000 year events were calculated for the Portsmouth tide gauge. For each event peak, two time series were created using the upper and lower storm-tide time series bounds for the Portsmouth site, defined in the analysis outlined in section 3.1. Each event time series was used as a water level boundary condition to force the inundation model for both the breach and no breach scenarios. The resulting inundation and property damages were then contrasted.

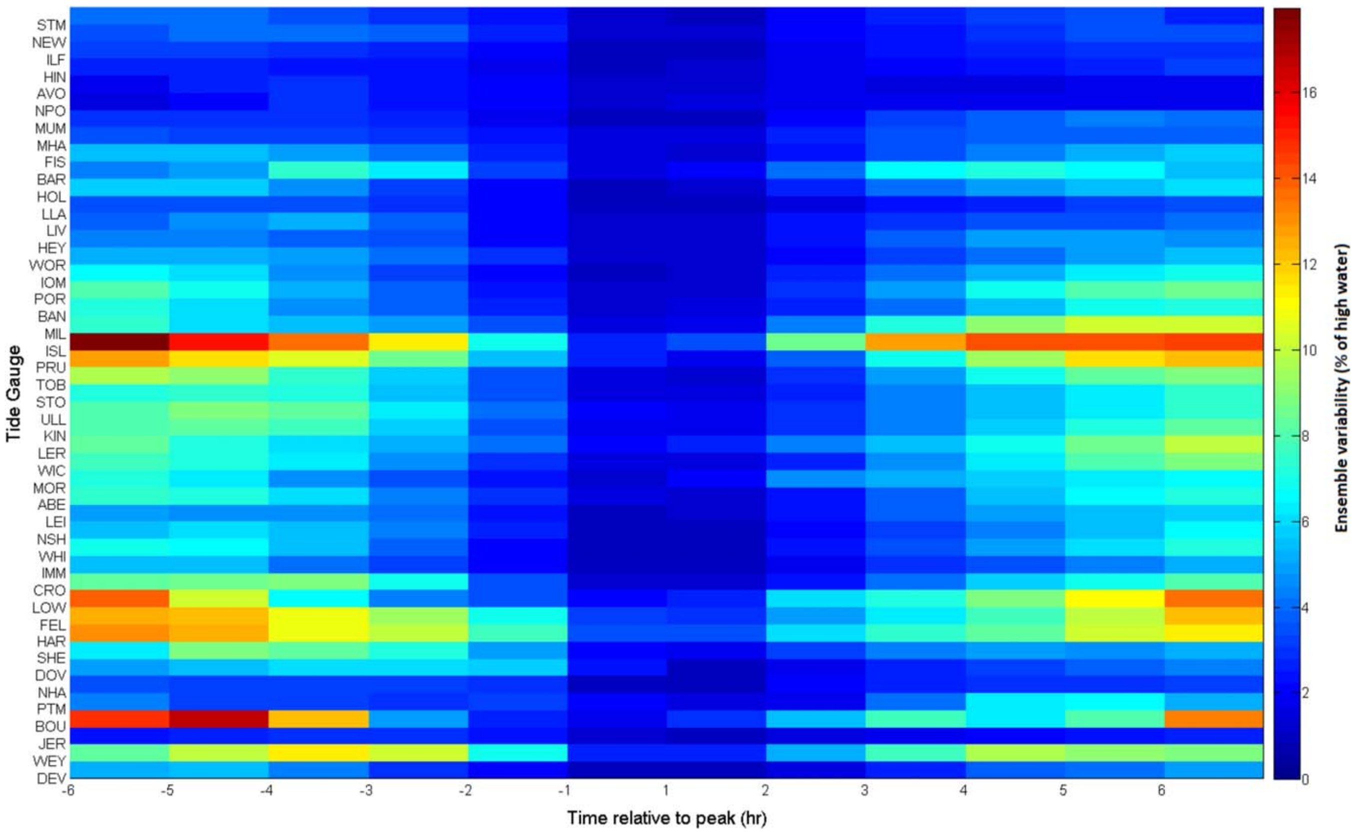

Figure 5. Standard deviation in water levels (% of high water) every hour relative to time of high water. Sites are ordered from (top) STM moving clockwise around the UK ending at DEV.

4. Results and Discussion

4.1. Variability in the Storm-Tide Event Time Series

Using the methods described in section 3.1, the variability in the measured storm-tide time series, tide, and nontidal components, was examined at each study site. Given the ensemble of events examined and the statistics extracted (section 3.1), variability was found in the tide and nontidal residual time series ensembles, and therefore, the resulting storm-tide time series, at each time step.

Using Felixstowe as an illustration, Figures 4a and 4b show the tidal time series ensembles, and the tidal time series ensembles where elevation is normalized relative to the high-tide magnitudes, respectively. Figures 4c and 4d show the nontidal residual time series ensembles, and the residual time series ensembles where elevation is normalized relative to the high water magnitudes, respectively. The variability in the time series of these signals, when comparing the ensembles of events, led to significant variability in the ensemble of the storm-tide time series at the tide gauges considered in this research (Figures 4e and 4f). Previous research [e.g., *McMillan et al*., 2011; *Batstone et al*., 2013] has also demonstrated that the magnitude of nontidal residuals at a given time relative to high water can differ considerably between events, with important implications upon the resulting storm-tide time series.

The time series variability at each site (defined by the standard deviation in the storm-tide elevation ensemble, every hour relative to the high water) is shown in Figure 5, while the event-mean (mean of all time steps) is plotted in Figure 6 for each site. The magnitude of the variability in the storm-tide time series ensemble at a given site varied with the time relative to high water, with an r^2 correlation of 0.98 when plotting the mean variability at each time step across all sites against the time from high water. This finding indicates that close to high water, variability in the time series between events is relatively low (e.g., commonly less than 1.5% and less than 3.6% within 1 h at all sites). Examination of the tidal time series

10.1002/2014JC010197

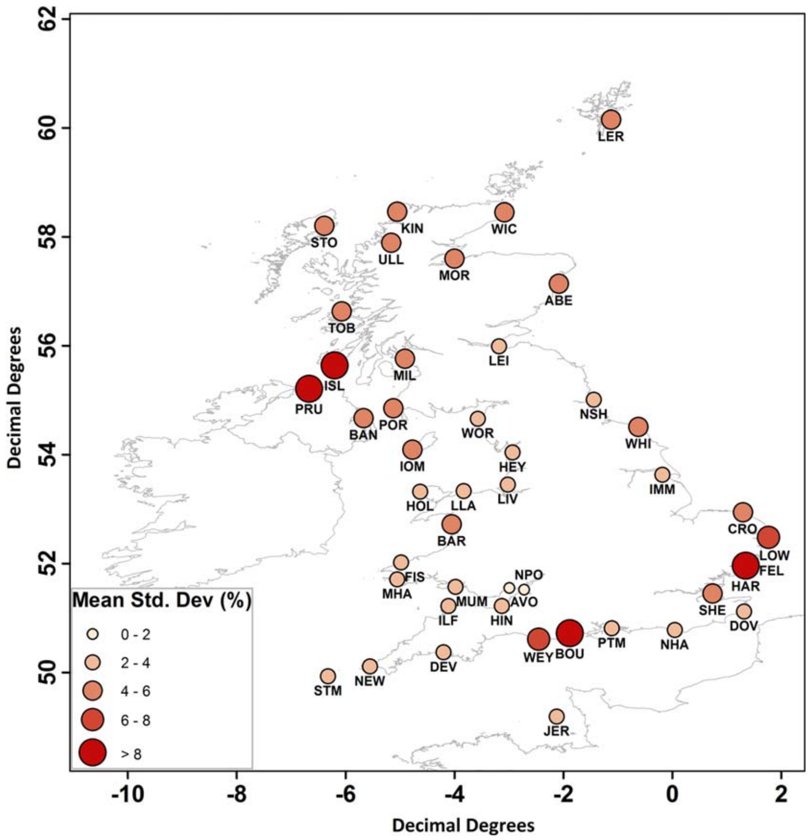

Figure 6. Event-mean standard deviation (variability) in water level time series.

ensembles at each site indicated that time series variability in tidal elevations, relative to the high water, increased away from high water (Figures 4a and 4b). This demonstrates that although the tide can be considered as relatively predictable, the time series of tidal cycles within the ensemble of events considered in this research will vary depending on the magnitude of the high tide. Furthermore, interactions between tides and surges have been shown to alter the wave phase speeds of both signals, often resulting in the clustering of nontidal residual peaks away from high water [*Horsburgh and Wilson*, 2007; *Howard et al.*, 2010]. This will be of particular importance to those interested in flood risk due to wave-overtopping and overflow of defenses, both of which are most likely to occur near to high water, and therefore, this portion of the storm-tide time series (and its uncertainty) will be of greatest importance to predictions of inundation depth and extent.

Comparison of the results at all UK gauges revealed that the magnitude of the variability in the storm-tide time series ensemble also differed significantly between sites. Given the event-mean variability in the water levels (the mean of all time steps) at each site (Figure 6), the results indicate that the magnitude of the variability in storm-tide time series across the UK ranged from 1.9% at Newport to 11.3% at Port Ellen, with a UK mean of 4.6%. Using Figure 6, regional characterizations can be made. For instance, the greatest mean variability in water level time series, when considered as a proportion of high water, was found in the northwest at sites such as Port Ellen and Portrush, and in the southeast at Harwich and Felixstowe. Alternatively, the southwest was shown to contain the least variability, the reasons for which are discussed below.

For context, given a 1 in 300 year event peak magnitude, the event-mean difference between the upper (95th) and lower (5th) bounds of the time series variability across all sites, in meters, was 0.95 m, with the largest and smallest differences occurring at Felixstowe (1.56 m) and Lerwick (0.59 m), respectively (Figure 7). Where only the high water ($\pm$3 h) of the time series was considered, all sites lay within 2 standard deviations of the UK mean, given as 0.17 m and 0.65 m, respectively, with the exception of Felixstowe, which had a larger mean difference between the two time series bounds than expected (1.1 m). All sites assessed

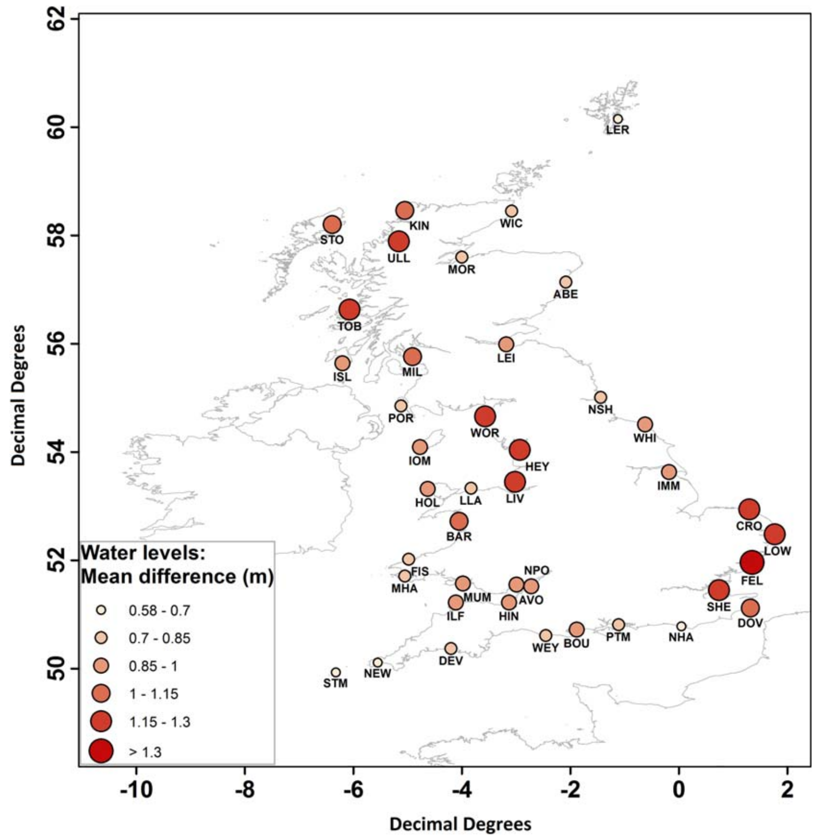

Figure 7. Event-mean difference in water levels at each site when contrasting the upper (95th) and lower (5th) time series bounds assigned to current 1 in 300 year storm tides.

showed a difference of at least 0.4 m between the upper and lower time series bounds within 3 h of high water.

The considerable differences in time series variability between the gauge sites are due to the differing tide and nontidal residual characteristics found around the UK [see *Pugh*, 1987]. For instance, plotting the event-mean time series variability against the ensemble mean tidal range at each site provided an r^2 correlation of 0.78 (Figure 8). This relationship was not unexpected given that in this research variability was normalized by the corresponding high water magnitude.

The magnitudes of the nontidal residuals at a site were also influential to the time series variability when considered in addition to the tidal range. The magnitude of the 99th percentile nontidal residual was found for each site and normalized by the corresponding ensemble mean tidal range. Plotting this new variable against the event-mean variability in the storm-tide ensembles at each site provided an r^2 correlation of 0.86 (Figure 8). This plot indicates that sites with relatively low tidal ranges and large nontidal residual magnitudes are likely to contain the greatest variability in the storm-tide time series when given as a proportion of the storm-tide peak elevation. Although small errors in the calculated nontidal residual may be present [see *Horsburgh and Wilson*, 2007], it is expected the 99th percentile magnitude used here is a suitable indicator of the difference in the nontidal component of the water levels between sites.

This correlation helps to explain why within the Severn Estuary the ensemble with the least variability in the ensemble of event time series was found. At Avonmouth, for example, although the 99th percentile nontidal residual magnitude was the largest of all the sites, the extremely large tidal range (exceeding 13 m) resulted in one of the smallest nontidal residual: tidal range ratios, and subsequently, one of the lowest scores for storm-tide time series variability. The opposite was found at sites such as Lowestoft and Port Ellen, where some of the smallest tidal ranges (due to their proximity to amphidromic points) coincided with relatively large 99th percentile nontidal residual magnitudes.

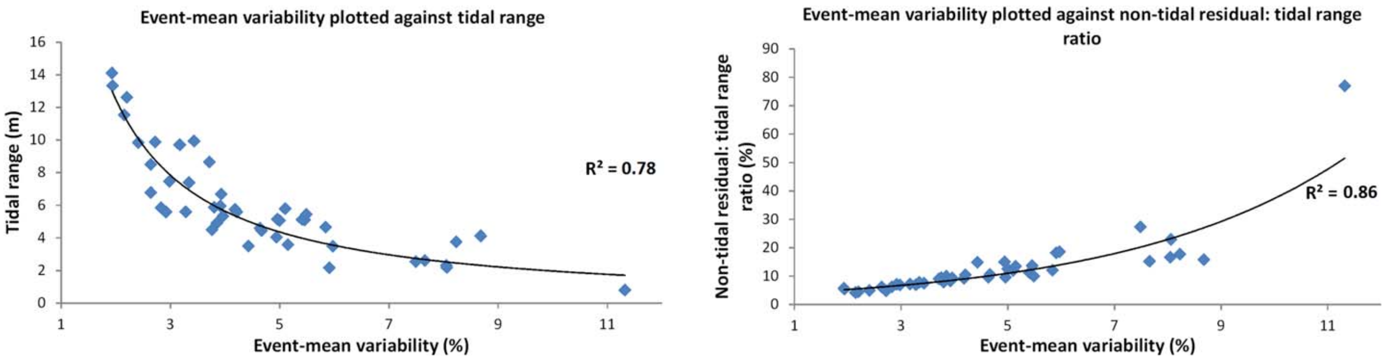

Figure 8. Correlation between event-mean time series variability at each site with (left) tidal range and (right) the nontidal residual magnitude normalized relative to the tidal range.

These findings demonstrate that when considering the largest 1% of events, there is variability in the time series of extreme storm tides recorded at all Class A tide gauges around the UK. The results presented also provide a valuable insight into how the magnitude of this variability changes spatially between tide gauge sites and temporally during an event. The envelopes of variability calculated at each site could be used in future probabilistic flood risk assessments to more accurately quantify the uncertainty in the model outputs due to assumptions commonly made about the time series of the storm-tide boundary conditions; currently not considered in most coastal flood risk studies. For instance, given a 1 in 300 year event peak magnitude at a given site, the upper and lower event time series bounds defined in this research could be used as boundary conditions to an inundation model. By simulating the model with both sets of boundary

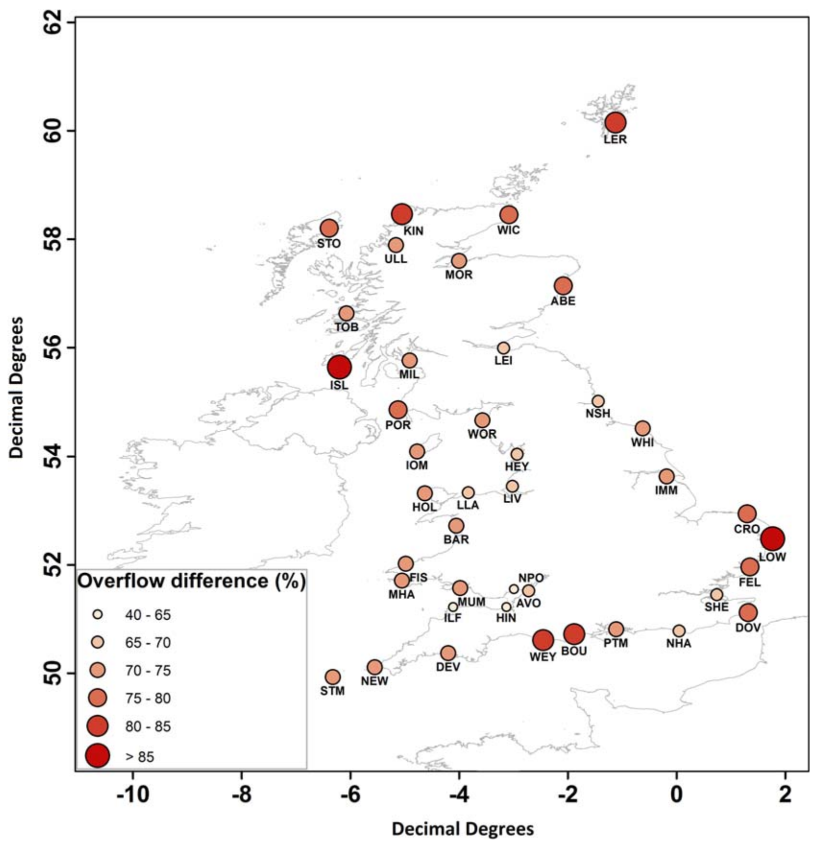

Figure 9. The difference in estimated overflow volumes per unit area of defense when contrasting the upper (95th) and lower (5th) time series bounds assigned to a 1 in 300 year storm tide at each site.

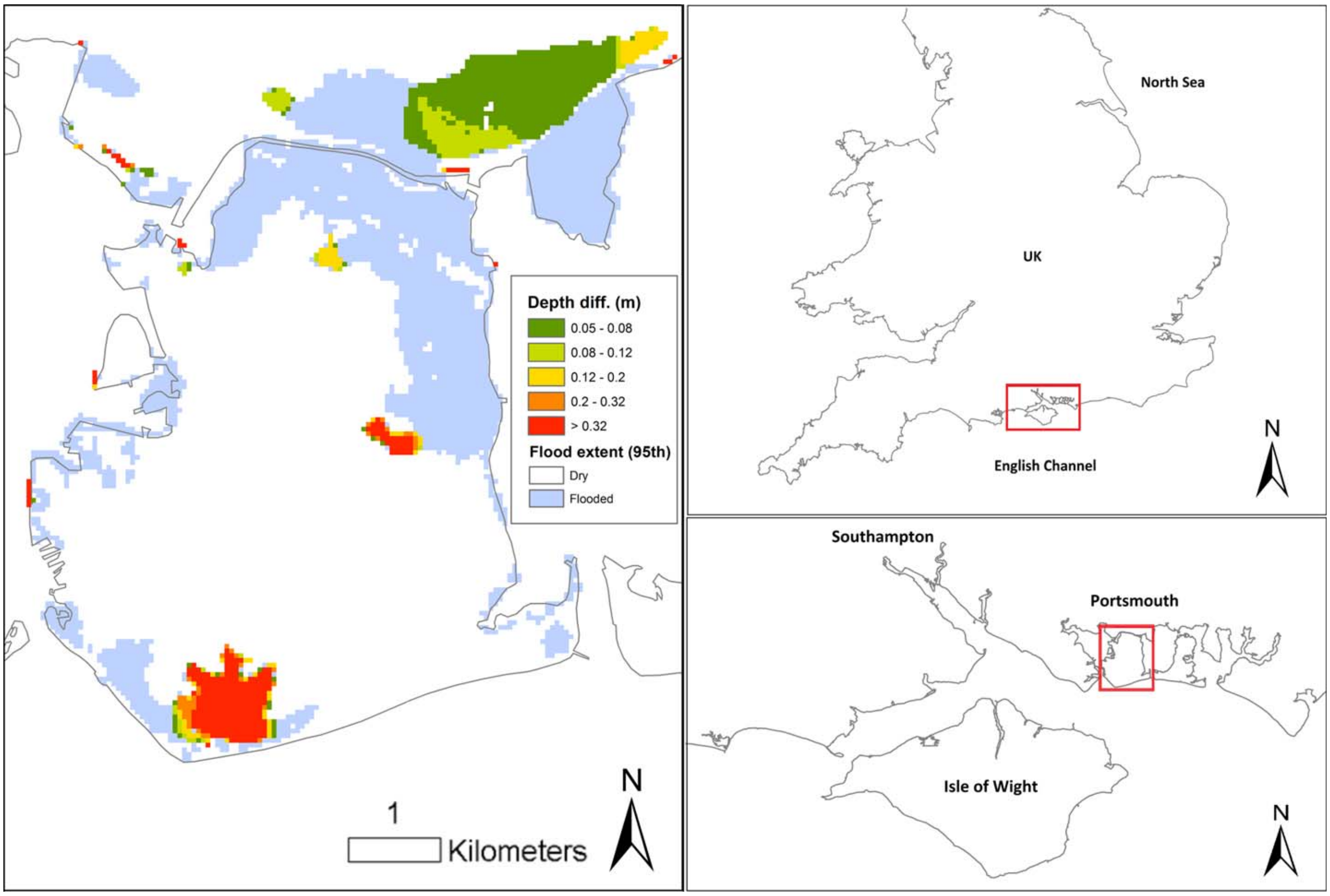

Figure 10. Flood simulation output for Portsmouth with a 1 in 1000 sea level and full breach scenario, and the difference in flood depths between the lower (5th) and upper (95th) percentile time series simulations.

conditions, the uncertainty in the prediction of coastal inundation due to uncertainty in an extreme event time series could be properly quantified. By describing these idealized time series as a proportion of the high water, the envelopes of variability defined may be applied to any given return period event of interest.

4.2. The Potential Impact Upon Coastal Inundation

The potential impacts of the variability discussed in section 4.1 upon coastal inundation predictions were examined using the methods and variability envelopes described in section 3.2. Given the differences in the storm-tide time series upper and lower bounds for the events described in section 3.2, the idealized defense overflow analysis (shown in Figure 9) indicated that there was considerable uncertainty in the predicted overflow volumes during an extreme event. Given a 1 in 300 year storm-tide event, the difference between overflow volumes estimated using the upper and lower bound time series ranged from 63% (Port Ellen) to 88% (Lowestoft), with a UK mean of 73%. The same analysis, considering 1 in 500 and 1 in 1000 year events indicated that the greatest uncertainty is likely to be during less severe events, for instance, where overflow of defenses occurs for a relatively short duration, due to the proportional assessment used. However, even during very extreme events the difference in predicted overflow volumes remained high. For instance, the mean difference in overflow volumes (given all sites) was 69% and 47% for the 1 in 500 and 1 in 1000 year events, respectively.

The case study assessment at Portsmouth provided a detailed insight into the consequences time series variability during storm-tide events might have upon flood risk predictions. Figure 10 demonstrates the difference in the predicted inundation depth and extent when using the defined upper and lower time series bounds, given a worst case (full breach) scenario during a 1 in 1000 year event. Table 2 provides the

Table 2. Simulated Inundation Characteristics for the Portsmouth Case Study

		Overflow		Breach of All Defenses	
	Return Period	Total	>1 m Depth	Total	>1 m Depth
Upper bound time series					
1 in 1	1	0	0	2786	97
1 in 10	10	0	0	5385	364
1 in 50	50	58	0	7264	1088
1 in 200	200	4409	184	9776	2301
1 in 300	300	4901	260	10,907	2649
1 in 500	500	5620	580	12,128	3220
1 in 1000	1000	6750	1520	13,156	3955
Lower bound time series					
1 in 1	1	0	0	2358	96
1 in 10	10	0	0	4644	232
1 in 50	50	57	0	6836	685
1 in 200	200	2974	86	8686	1522
1 in 300	300	3651	119	9188	1846
1 in 500	500	4376	125	10,229	2417
1 in 1000	1000	6201	721	11,762	3135

results from each simulation. As expected, the variability in the time series of a given event had a clear effect upon the expected inundation of the region due to the duration and magnitude by which defenses were exceeded. For example, where defenses were held, the implementation of the upper (95th percentile) time series to the 1 in 1000 year event water level resulted in a 8% increase in the expected number of properties inundated and a 53% increase in those experiencing depths greater than 1 m relative to prediction made using the lower (5th percentile) time series.

These findings indicate that storm-tide time series temporal variability is likely to be a significant source of uncertainty to flood risk assessments, particularly within quantification of consequences for extreme sea level and defense exceeding events; due to both the size of the uncertainty in the volume of water entering the domain and the sensitivity of commonly used inundation models to this input. Therefore, this should be accounted for in such scenarios using the methods described in this research.

5. Conclusions

This research has demonstrated that there is considerable variability in the hours leading up to and proceeding the maximum water levels experienced during extreme storm-tide events, which can influence flood risk assessment. This variability has been quantified relative to a given storm-tide peak, for each gauge, based upon the analysis of extreme (>1%) water levels since 1993. The findings demonstrated that the magnitude of the event-mean time series variability across the gauges assessed ranged from 1.9% to 11.3%, with a UK average of 4.6%. Given a 1 in 300 year event, the comparison between the upper and lower bounds of storm-tide variability at each site resulted in an event-mean difference of 0.95 m when considering all UK gauges. Although the magnitude of the variability was usually greatest during the low water; all sites contained a difference of at least 0.4 m when considering the time series variability within 3 h of high water. The greatest variability was found to occur at sites experiencing relatively low tidal ranges and large nontidal residuals, such as Felixstowe and Harwich in the southern North Sea.

Assuming coastal defenses built to a 1 in 200 year capacity, the difference in overflow volume during a 1 in 200, 500 and 1000 year event, due to the time series variability at each site, was examined. The results revealed that this variability resulted in a UK average difference of 73%, 69%, and 47% in the event-mean estimated overflow volumes for the 1 in 200, 500, and 1000 year events, respectively. A detailed case study at Portsmouth further demonstrated the importance of quantifying the variability in storm-tide time series for flood risk assessments, considering a range of storm-tide magnitudes. Given a current 1 in 200 year event, the difference between the upper and lower bounds of the storm-tide variability resulted in an increase of more than 30% in the number of buildings expected to be inundated in the region. It is therefore relevant that other case studies should be explored, while it is also recommended that future inundation modeling (whether deterministic or probabilistic) adequately represents this source of uncertainty when defining inundation exposure and consequences.

Future research could extend the analysis to consider other coastal processes of relevance to flood risk that might be impacted by time series variability, such as wave-overtopping, sediment transportation, or defense failure. For instance, it would be expected that the duration of high water would influence the volume of wave-overtopping a section of defense might experience, while also impacting the likelihood of defense failure due to changes in the wave loading. Similarly the time series uncertainty may have significant impacts upon the predicted erosion of soft coastal defenses or offshore sand banks due to the influence of water depth and wave forcing on the geomorphology of such features. For these reasons, investigation of the effects to coastal flood risk estimates due to uncertainty with a storm-tide time series when applied to a multimodel system [such as the defense overtopping-defense breaching model of *Wood and Bateman*, 2005] would be particularly valuable to coastal managers.

Acknowledgments
The research presented in this paper was funded by the KULTURisk FP7-ENV-2010 project, while M.P. Wadey and I.D. Haigh time was funded by the NERC Flood Memory EP/K013513/1 project. The authors are grateful to the National Tidal and Sea Level Facility (hosted by the National Oceanographic Centre) and the British Oceanographic Data Centre for the provision of the UK tide gauge data used in this research. The data for this paper can be obtained from the British Oceanographic Data Centre at https://www.bodc.ac.uk/data/online_delivery/ntslf/processed/.

References

Ackers, P., W. R. White, J. A. Perkins, and A. J. M. Harrison (1978), *Weirs and Flumes for Flow Measurement*, John Wiley, Chichester, U. K.

Barmania, S. (2014), Typhoon Haiyan recovery: Progress and challenges, *Lancet*, *383*(9924), 1197–1199, doi:10.1016/S0140-6736(14)60590-0.

Bates, P. D., R. J. Dawson, J. W. Hall, M. S. Horritt, R. J. Nicholls, J. Wicks, and H. Mohamed Ahmed Ali Mohamed (2005), Simplified two-dimensional numerical modelling of coastal flooding and example applications, *Coastal Eng.*, *52*, 793–810, doi:10.1016/j.coastaleng.2005.06.001.

Bates, P. D., M. S. Horritt, and T. J. Fewtrell (2010), A simple inertial formulation of the shallow water equations for efficient two-dimensional flood inundation modelling, *J. Hydrol.*, *387*, 33–45, doi:10.1016/j.jhydrol.2010.03.027.

Batstone, C., M. Lawless, J. Tawn, K. Horsburgh, D. Blackman, A. McMillan, D. Worth, S. Laeger, and T. Hunt (2013), A UK best-practice approach for extreme sea-level analysis along complex topographic coastlines, *Ocean Eng.*, *71*, 28–39, doi:10.1016/j.oceaneng.2013.02.003.

Baxter, P. J. (2005), The east coast Big Flood, 31 January–1 February 1953: A summary of the human disaster, *Philos. Trans. R. Soc. A*, *363*, 1293–1312, doi:10.1098/rsta.2005.1569.

Bocquet, F., J. Flowerdew, P. Hawkes, T. Pullen, and N. Tozer (2009), Probabilistic coastal flood forecasting: Forecast demonstration and evaluation, *Environ. Agency Rep. SC050089*, Environment Agency, Bristol. [Available at http://cdn.environment-agency.gov.uk/scho0109bpfp-e-e.pdf.]

Brown, J., R. Bolanos, and J. Wolf (2011), Impact assessment of advanced coupling features in a tide-surge-wave model, POLCOMS-WAM, in a shallow water application, *J. Mar. Syst.*, *87*(1), 13–24, doi:10.1016/j.jmarsys.2011.02.006.

Brown, J. D., and S. L. Damery (2002), Managing flood risk in the UK: Towards an integration of social and technical perspectives, *Trans. Inst. Br. Geogr.*, *27*(4), 412–426, doi:10.1111/1475-5661.00063.

Brown, J. D., T. Spencer, and I. Moeller (2007), Modeling storm surge flooding of an urban area with particular reference to modeling uncertainties: A case study of Canvey Island, United Kingdom, *Water Resour. Res.*, *43*, W06402, doi:10.1029/2005WR004597.

Committee on Climate Change (2013), Managing the land in a changing climate—Adaptation sub-committee progress report 2013. [Available at http://www.theccc.org.uk/publication/managing-the-land-in-a-changing-climate/.]

Davis, J., V. Paramygin, D. Forrest, and Y. Sheng (2010), Toward the probabilistic simulation of storm surge and inundation in a limited resource environment, *Mon. Weather Rev.*, *138*, 2953–2974, doi:10.1175/2010MWR3136.1.

Dawson, R., J. Hall, P. Sayers, and P. Bates (2003), Flood risk assessment for shoreline management planning, in *Proceedings of the International Conference on Coastal Management*, edited by R. G. McInnes, pp. 83–97, Thomas Telford, London, U. K.

Dawson, R. J., J. W. Hall, P. D. Bates, and R. J. Nicholls (2005), Quantified analysis of the probability of flooding in the Thames Estuary under imaginable worst-case sea level rise scenarios, *Water Resour. Dev.*, *21*, 577–591, doi:10.1080/07900620500258380.

Dawson, R. J., et al. (2009), Integrated analysis of coastal flooding and cliff erosion under scenarios of long term change, *Clim. Change*, *95*, 249–288, doi:10.1007/s10584-008-9532-8.

Fewtrell, T. J., P. D. Bates, M. Horritt, and N. M. Hunter (2008), Evaluating the effect of scale in flood inundation modelling in urban environments, *Hydrol. Processes*, *22*, 5107–5118, doi:10.1002/hyp.7148.

Flather, R. (1994), A storm surge prediction model for the Northern Bay of Bengal with application to the cyclone disaster in April 1991, *J. Phys. Oceanogr.*, *24*(1), 172–190, doi:10.1175/1520-0485(1994)024<0172:ASSPMF>2.0.CO;2.

Flowerdew, J., K. Horsburgh, and K. Mylne (2009), Ensemble forecasting of storm surges, *Mar. Geod.*, *32*(2), 91–99, doi:10.1080/01490410902869151.

Gallien, T. W., J. E. Schubert, and B. F. Sanders (2011), Predicting tidal flooding of urbanized embayments: A modeling framework and data requirements, *Coastal Eng.*, *58*, 567–577, doi:10.1016/j.coastaleng.2011.01.011.

Gerritsen, H. (2005), What happened in 1953? The big flood in the Netherlands in retrospect, *Philos. Trans. R. Soc. A*, *363*, 1271–1291, doi:10.1098/rsta.2005.1568.

Gönnert, G. M., S. K. Dube, T. S. Murty, and W. Siefert (2001), *Global Storm Surges: Theory Observation and Application*, vol. 63, Boyens, Heide i. Holstein, Germany.

Haigh, I. D., R. Nicholls, and N. Wells (2010), A comparison of the main methods for estimating probabilities of extreme still water levels, *Coastal Eng.*, *57*, 838–849, doi:10.1016/j.coastaleng.2010.04.002.

Haigh, I., R. Nicholls, and N. Wells (2011), Rising sea levels in the English Channel 1900 to 2100, *Proc. ICE Mar. Eng.*, *164*(2), 81–92, doi:10.1680/maen.2011.164.2.81.

Haigh, I. D., L. R. MacPherson, M. S. Mason, E. M. S. Wijeratne, C. B. Pattiaratchi, and S. George (2014a), Estimating present day extreme water level exceedance probabilities around the coastline of Australia: Tropical cyclone induced storm surges, *Clim. Dyn.*, *42*(1–2), 139–157, doi:10.1007/s00382-012-1653-0.

Haigh, I. D., E. M. S. Wijeratne, L. R. MacPherson, C. B. Pattiaratchi, M. S. Mason, R. P. Crompton, and S. George (2014b), Estimating present day extreme total water level exceedance probabilities around the coastline of Australia: Tides, extra-tropical storm surges and mean sea level, *Clim. Dyn.*, *42*(1–2), 121–138, doi:10.1007/s00382-012-1652-1.

Hall, J., and D. Solomatine (2008), A framework for uncertainty analysis in flood risk management decisions, *Int. J. River Basin Manage.*, *6*(2), 85–98, doi:10.1080/15715124.2008.9635339.

Horsburgh, K., and C. Wilson (2007), Tide-surge interaction and its role in the distribution of surge residuals in the North Sea, *J. Geophys. Res.*, *112*, C08003, doi:10.1029/2006JC004033.

Horsburgh, K., J. A. Williams, J. Flowerdew, and K. Mylne (2008), Aspects of operational forecast model skill during an extreme storm surge event, *J. Flood Risk Manage.*, *1*(4), 213–221, doi:10.1111/j.1753-318X.2008.00020.x.

Houghton, J. (2005), Global warming, *Rep. Prog. Phys.*, *68*, 1343–1403, doi:10.1088/0034-4885/68/6/R02.

Howard, T., J. Lowe, and K. Horsburgh (2010), Interpreting century-scale changes in southern North Sea storm surge climate derived from coupled model simulations, *J. Clim.*, *23*(23), 6234–6247, doi:10.1175/2010JCLI3520.1.

Hunt, J. (2005), Inland and coastal flooding: Developments in prediction and prevention, *Philos. Trans. R. Soc. A*, *363*, 1475–1491, doi:10.1098/rsta.2005.1580.

Kantha, L., and C. Clayson (2000), *Numerical Models of Oceans and Oceanic Processes*, Academic, San Diego, Calif.
Kim, S., T. Yasuda, and H. Mase (2010), Wave set-up in the store surge along open coasts during Typhoon Anita, *Coastal Eng.*, *57*, 631–642, doi:10.1016/j.coastaleng.2010.02.004.
Lewis, M., K. Horsburgh, P. Bates, and R. Smith (2011), Quantifying the uncertainty in future coastal flood risk estimates for the U.K., *J. Coastal Res.*, *27*, 870–881, doi:10.2112/JCOASTRES-D-10-00147.1.
Lewis, M., G. Schumann, P. Bates, and K. Horsburgh (2013), Understanding the variability of an extreme storm-tide along a coastline, *Estuarine Coastal Shelf Sci.*, *123*, 19–25, doi:10.1016/j.ecss.2013.02.009.
Lowe, J. A., et al. (2009), *UK Climate Projections Science Report: Marine and Coastal Projections*, Met Off. Hadley Cent., Exeter, U. K. [Available at http://academia.edu/1892600/UK_Climate_Projections_science_report_Marine_and_coastal_projections.]
Madsen, H., and R. Canizares (1999), Comparison of extended and ensemble Kalman Filters for data assimilation in coastal area modelling, *Int. J. Numer. Methods Fluids*, *31*, 961–981, doi:10.1002/(SICI)1097-0363(19991130)31:6<961::AID-FLD907>3.3.CO;2-S.
Maybeck, P. (1979), *Stochastic Models, Estimation and Control*, vol. 1, Academic, N. Y.
McCabe, M., P. Stansby, and D. Apsley (2013), Random wave runup and overtopping a steep wall: Shallow-water and Boussinesq modelling with generalised breaking and wall impact algorithms validated against laboratory and field measurements, *Coastal Eng.*, *74*, 33–49, doi:10.1016/j.coastaleng.2012.11.010.
McMillan, A., C. Batstone, D. Worth, J. Tawn, K. Horsburgh, and M. Lawless (2011), *Coastal Flood Conditions for UK Mainland and Islands, Project SC060064/TR2: Design Sea Levels*, 142 pp., Environ. Agency, Bristol, U. K.
McRobie, A., T. Spencer, and H. Gerritsen (2005), The Big Flood: North Sea storm surge, *Philos. Trans. R. Soc. A*, *363*, 1263–1270, doi:10.1098/rsta.2005.1567.
Meehl, G. A., et al. (2007), *Global Climate Projections. In Climate Change 2007: The Physical Science Basis. Contribution of Working Group I to the Fourth Assessment Report of the Intergovernmental Panel on Climate Change*, edited by S. Solomon et al., Cambridge University Press, Cambridge, U. K. [Available at http://www.ipcc.ch/publications_and_data/publications_ipcc_fourth_assessment_report_wg1_report_the_physical_science_basis.htm.]
Mokrech, M., R. J. Nicholls, and R. J. Dawson (2012), Scenarios of future built environment for coastal risk assessment of climate change using a GIS-based multicriteria analysis, *Environ. Plann. B: Plann. Design*, *39*(1), 120–136, doi:10.1068/b36077.
Neal, J. (2007), Flood forecasting and adaptive sampling with spatially distributed dynamic depth sensors, PhD thesis, Univ. of Southampton, Southampton, U. K.
Nicholls, R. J. (1995), Coastal megacities and climate change, *GeoJournal*, *37*, 369–379, doi:10.1007/BF00814018.
Pappenberger, F., and K. J. Beven (2006), Ignorance is bliss: Or seven reasons not to use uncertainty analysis, *Water Resour. Res.*, *42*, W05302, doi:10.1029/2005WR004820.
Pawlowicz, R., B. Beardsley, and S. Lentz (2002), Classical tidal harmonic analysis with errors in matlab using t-tide, *Comput. Geosci.*, *28*, 929–937, doi:10.1016/S0098-3004(02)00013-4.
Pugh, D. J. (1987), *Tides, Surges and Mean Sea-level. A Handbook for Engineers and Scientists*, 472 pp., John Wiley, Chichester, U. K.
Pugh, D. J. (2004), *Changing Sea Levels: Effects of Tides, Weather and Climate*, Cambridge University Press, Cambridge, U. K.
Pullen, T., N. W. H. Allsop, T. Bruce, A. Kortenhaus, H. Schuttrumpf, and J. van der Meer (2007), Eurotop, wave overtopping of sea defences and related structures—Assessment manual Die Küste, Heft 73. [Available at http://www.overtopping-manual.com/manual.html.]
Pullen, T., W. Allsop, T. Bruce, and J. Pearson (2009), Field and laboratory measurements of mean overtopping discharges and spatial distributions at vertical seawalls, *Coastal Eng.*, *56*, 121–140, doi:10.1016/j.coastaleng.2008.03.011.
Purvis, M., P. Bates, and C. Hayes (2008), A probabilistic methodology to estimate future coastal flood risk due to sea level rise, *Coastal Eng.*, *55*, 1062–1073, doi:10.1016/j.coastaleng.2008.04.008.
Quinn, N., P. D. Bates, and M. Siddall (2013), The contribution to future flood risk in the Severn Estuary from extreme sea level rise due to ice sheet mass loss, *J. Geophys. Res. Oceans*, *118*, 5887–5898, doi:10.1002/jgrc.20412.
RIBA, and ICE (2009), *Facing up to Rising Sea-Levels: Retreat? Defend? Attack? The Future of Our Coastal and Estuarine Cities*, London. [Available at http://www.buildingfutures.org.uk/assets/downloads/Facing_Up_To_Rising_Sea_Levels.pdf.]
Risk Management Solutions (2005), *Hurricane Katrina: Profile of a Super Cat, Lessons and Implications for Catastrophic Risk Management*, Risk Manage. Solutions, Newark, Calif. [Available at https://support.rms.com/publications/KatrinaReport_LessonsandImplications.pdf.]
Roelvink, D., A. Reniers, A. van Dongeren, J. van Thiel de Vries, R. McCall, and J. Lescinski (2009), Modelling storm impacts on beaches, dunes and barrier islands, *Coastal Eng.*, *56*, 1133–1152, doi:10.1016/j.castaleng.2009.08.006.
Sekovski, I., A. Newton, and W. C. Dennison (2012), Megacities in the coastal zone: Using a driver-pressure-state-impact-response framework to address complex environmental problems, *Estuarine Coastal Shelf Sci.*, *96*, 48–59, doi:10.1016/j.ecss.2011.07.011.
Slingo, J., et al. (2014), The recent storms and floods in the UK, Met Office, Exeter, U. K. [Available at http://www.metoffice.gov.uk/media/pdf/1/2/Recent_Storms_Briefing_Final_SLR_20140211.pdf.]
Small, C., and R. J. Nicholls (2003), A global analysis of human settlement in coastal zones, *J. Coastal Res.*, *19*(3), 584–599. [Available at ftp://ftp.ldeo.columbia.edu/pub/small/PUBS/SmallNichollsJCR2003.pdf.]
Smith, R., P. Bates, and C. Hayes (2012), Evaluation of a coastal flood inundation model using hard and soft data, *Environ. Modell. Software*, *30*, 35–46, doi:10.1016/j.envsoft.2011.11.008.
Spencer, T., and J. French (1993), Coastal flooding: Transient and permanent, *Geography*, *78*(2), 179–182. [Available at http://www.jstor.org/stable/40572502.]
Stansby, P., et al. (2012), An integrated model system for coastal flood prediction with a case history for Walcott, UK, on 9 November 2007, J. Flood Risk Manage., *6*(3), 229–252, doi:10.1111/jfr3.12001.
Tawn, J. A. (1992), Estimating probabilities of extreme sea levels, *Appl. Stat.*, *41*, 77–93, doi:10.2307/2347619.
Tibbetts, J. (2002), Coastal cities: Living on the edge, *Environ. Health Perspect.*, *110*(11), A674–A681, doi:10.1289/ehp.110-a674.
Turner, R. K., S. Subak, and W. N. Adger (1996), Pressures, trends, and impacts in coastal zones: Interactions between socioeconomic and natural systems, *Environ. Manage.*, *20*, 159–173, doi:10.1007/BF01204001.
Wadey, M., R. Nicholls, and C. Hutton (2012), Coastal flooding in the Solent: An integrated analysis of defences and inundation, *Water*, *4*, 430–459, doi:10.3390/w4020430.
Wadey, M. P., R. J. Nicholls, and I. Haigh (2013), Understanding a coastal flood event: The 10th March 2008 storm surge event in the Solent, UK, *Nat. Hazards*, *67*(2), 1–26, doi:10.1007/s11069-013-0610-5.
Wolf, J. (2009), Coastal flooding: Impacts of coupled wave-surge-tide models, *Nat. Hazards*, *49*(2), 241–260, doi:10.1007/s11069-008-9316-5.
Wood, R. M., and W. Bateman (2005), Uncertainties and constraints on breaching and their implications for flood loss estimation, *Phil. Trans. R. Soc. A*, *15, 363, 1831*, 1423–1430, doi:10.1098/rsta.2005.1576.
Zong, Y., and M. Tooley (2003), A historical record of coastal floods in Britain: Frequencies and associated storm tracks, *Nat. Hazards*, *29*, 13–36, doi:10.1023/A:1022942801531.

